The Tol-Pal system is required for peptidoglycan-cleaving enzymes to complete bacterial cell division

Anastasiya A. Yakhnina[a] and Thomas G. Bernhardt[a,b,1]

[a]Department of Microbiology, Harvard Medical School, Boston, MA 02115; and [b]Howard Hughes Medical Institute, Boston, MA 02115

Edited by Thomas J. Silhavy, Princeton University, Princeton, NJ, and approved February 11, 2020 (received for review November 3, 2019)

Tol-Pal is a multiprotein system present in the envelope of Gram-negative bacteria. Inactivation of this widely conserved machinery compromises the outer membrane (OM) layer of these organisms, resulting in hypersensitivity to many antibiotics. Mutants in the *tol-pal* locus fail to complete division and form cell chains. This phenotype along with the localization of Tol-Pal components to the cytokinetic ring in *Escherichia coli* has led to the proposal that the primary function of the system is to promote OM constriction during division. Accordingly, a poorly constricted OM is believed to link the cell chains formed upon Tol-Pal inactivation. However, we show here that cell chains of *E. coli tol-pal* mutants are connected by an incompletely processed peptidoglycan (PG) layer. Genetic suppressors of this defect were isolated and found to overproduce OM lipoproteins capable of cleaving the glycan strands of PG. Among the factors promoting cell separation in mutant cells was a protein of previously unknown function (YddW), which we have identified as a divisome-localized glycosyl hydrolase that cleaves peptide-free PG glycans. Overall, our results indicate that the cell chaining defect of Tol-Pal mutants cannot simply be interpreted as a defect in OM constriction. Rather, the complex also appears to be required for the activity of several OM-localized enzymes with cell wall remodeling activity. Thus, the Tol-Pal system may play a more general role in coordinating OM invagination with PG remodeling at the division site than previously appreciated.

peptidoglycan | divisome | colicin | cell wall

During bacterial cell division, multiple layers of peptidoglycan (PG) are thought to be synthesized between the invaginating bilayers of the cytoplasmic membrane (1). This so-called septal PG connects the developing daughter cells. In most cases, this connection is temporary, and the daughters are separated by cleavage of the shared PG septum (2). This splitting process must be carefully controlled so that the new cell poles are formed without inducing lysis of one or both of the offspring (3). Gram-negative bacteria face an additional challenge of coordinating the constriction of the outer membrane (OM) with septal PG splitting and the invagination of the inner (cytoplasmic) membrane (IM) (4). These major cell envelope remodeling events are orchestrated by the cytokinetic ring organelle often referred to as the divisome or septal ring.

The divisome is organized by the tubulin-like FtsZ protein, which forms cytomotive filaments that treadmill about the prospective division site just underneath the IM (5–7). These filaments recruit a number of proteins to midcell, including the PG synthases that produce the septal PG matrix (1). IM invagination is most likely promoted by the process of septal PG biogenesis exerting an inward pushing force on the membrane, although a constrictive force of FtsZ filaments themselves has also been implicated (8). Septal PG splitting is catalyzed by enzymes called PG hydrolases that cleave bonds in the PG network. In *Escherichia coli* and other Gram-negative bacteria, LytC-type *N*-acetylmuramyl-L-alanine amidases play major role in the splitting process (2). These hydrolases cleave the linkage between the stem peptide and the glycan backbone of PG to break cross-links in the matrix and generate peptide-free (denuded) glycan strands. *E. coli* encodes three periplasmic amidases (AmiA, AmiB, and AmiC) and two amidase activators (EnvC and NlpD) that are critical for septal PG splitting (2, 9). EnvC is associated with the IM and activates AmiA and AmiB, whereas the OM lipoprotein NlpD serves as the activator for AmiC (10). Simultaneous inactivation of all three amidases or both of the activators leads to a severe cell separation defect, with mutants forming long chains of cells connected by unsplit septa and a shared OM (2, 9).

The factors within the divisome that promote OM constriction have not been clearly defined, but the Tol-Pal system is thought to play a major role in the process (4, 11). The system consists of an IM motor complex of TolQ, TolR, and TolA (TolQRA), the periplasmic protein TolB, and the PG-binding OM lipoprotein Pal (4). Mutants inactivating the system were first identified based on its role in the import of protein toxins called colicins across the OM (12). Subsequently, the loss of Tol-Pal activity was shown to have pleiotropic OM defects, including impairment of the OM permeability barrier, as evidenced by hypersensitivity of *tol-pal* mutants to detergents and large antibiotics, and the copious production of OM vesicles (13–17). Loss of Tol-Pal function in several Gram-negative bacteria, including *E. coli*, has also been found to result in a cell chaining phenotype (11, 15, 16, 18, 19). Coupled with localization studies indicating that the Tol-Pal proteins are recruited to the divisome, this latter phenotype has led to the widely accepted model that the major physiological role of the Tol-Pal system is to promote OM constriction during cell division (11, 20, 21).

We recently connected Tol-Pal function with the septal PG splitting process in *E. coli* (22). When combined with an *envC* deletion, inactivation of the Tol-Pal system was found to cause a severe cell chaining defect resembling that of an *envC nlpD* double mutant. This result suggested that Tol-Pal function may be required for amidase activation by NlpD, thus prompting us to further investigate the role of the Tol-Pal system in cell separation. Here,

Significance

The outer membrane of gram-negative bacteria presents a formidable barrier for the entry of antibiotics and is a significant contributor to the intrinsic drug resistance of these organisms. The highly conserved Tol-Pal complex has long been known to be required for the proper biogenesis of this surface layer, with its main function commonly believed to be promoting outer membrane constriction during cell division. In this report, we show that the machinery is needed to promote the cleavage of cell wall glycans at the division site to promote daughter cell separation. Thus, the Tol-Pal system may play multiple roles during cell division to ensure that outer membrane invagination and cell wall processing are properly coordinated.

Author contributions: A.A.Y. and T.G.B. designed research; A.A.Y. performed research; A.A.Y. and T.G.B. analyzed data; and A.A.Y. and T.G.B. wrote the paper.

The authors declare no competing interest.

This article is a PNAS Direct Submission.

[1]To whom correspondence may be addressed. Email: thomas_bernhardt@hms.harvard.edu.

This article contains supporting information online at https://www.pnas.org/lookup/suppl/doi:10.1073/pnas.1919267117/-/DCSupplemental.

First published March 9, 2020.

we show that the cell chaining phenotype caused by the inactivation of the Tol-Pal system alone is the result of a failure in septal PG splitting. Genetic suppressors indicate that, rather than resulting from a defect in NlpD and amidase activation, this phenotype is due to the reduced activity of OM lipoproteins capable of cleaving the glycan strands of PG. Among the factors promoting cell separation in the *tol-pal* mutant cells was YddW, which we have found to be a divisome-localized glycosyl hydrolase specific for denuded PG and, therefore, renamed it DigH. Overall, our results indicate that the cell chaining defect of Tol-Pal mutants cannot be merely interpreted as a defect in OM constriction. Rather, the system appears to be required for the activity of several OM-localized enzymes with cell wall remodeling activity. Thus, the Tol-Pal machinery may play a more general role in coordinating OM invagination with PG remodeling at the division site than previously appreciated.

Results

Cells Inactivated for Tol-Pal Have a Septal PG Splitting Defect. *E. coli* cells with a defective Tol-Pal system grow as long chains when they are cultured in low-salt medium (11, 18). This phenotype has been interpreted to result from a defect in OM constriction. However, electron micrographs available in the literature do not give a clear picture of whether the defect is restricted to OM constriction or stems from problems with septal PG splitting (15, 23). To distinguish between these possibilities, WT cells along with mutants deleted for the *tolQRA* operon (Δ*tolQRA*) or the entire *tolQRA-tolB-pal* locus (Δ*tol-pal*) were grown in lysogeny broth (LB) without NaCl (LB0N) in the presence of the fluorescent D-amino acid HADA (24) to label their PG. We then purified PG sacculi from these cells and visualized them by phase-contrast and fluorescence microscopy (Fig. 1 and *SI Appendix*, Fig. S1). As expected from previous results, intact cells of both the Δ*tolQRA* and Δ*tol-pal* mutants grew as cell chains (*SI Appendix*, Fig. S1). Notably, Δ*tolQRA* cells formed longer chains than those of the Δ*tol-pal* mutant, indicating that defects in the motor alone cause a more severe cell division defect than removal of the entire system (see below). Nevertheless, in both cases, the sacculi purified from these cells retained a chain-like morphology (Fig. 1 and *SI Appendix*, Fig. S1). This observation is indicative of a defect in septal PG splitting (*SI Appendix*, Fig. S1*A*), suggesting that the Tol-Pal system is required for proper PG remodeling at the division site in addition to its proposed role in OM constriction.

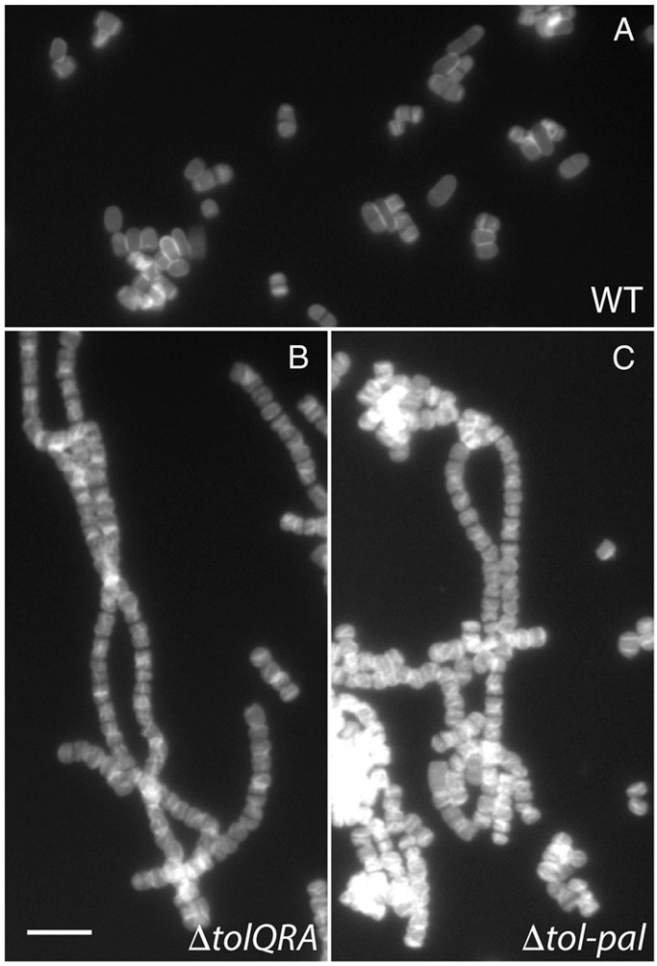

Fig. 1. Disruption of Tol-Pal leads to a septal PG splitting defect. Images of HADA labeled PG sacculi isolated from TB28 (WT) (*A*), AA40 (Δ*tolQRA*) (*B*), and MT91 (Δ*tol-pal*) (*C*) cells grown at 42 °C in the presence of 500 μM HADA for 3 h. Larger fields of view are presented in *SI Appendix*, Fig. S1. (Scale bar: 5 μm.)

Inactivation of Prc Suppresses the Division Phenotype of *tol-pal* Mutants. To investigate the nature of the septal PG splitting problem in Δ*tol-pal* mutants, we searched for suppressors that alleviated this defect. For this analysis, we took advantage of the severe growth defect of Tol-Pal defective cells on LB0N at 42 °C (Fig. 2*A*). Spontaneous survivors of this nonpermissive growth condition were isolated at a frequency of $\sim 4 \times 10^{-6}$. The isolates were then tested for suppression of cell chaining. Five suppressors were identified that grew on LB0N at 42 °C and displayed a relatively normal cell division phenotype (Fig. 2 *A* and *B*). Notably, these suppressors also had a partially restored OM permeability barrier indicated by increased resistance to vancomycin (*SI Appendix*, Fig. S2), to which Δ*tol-pal* mutants are normally hypersensitive (17).

Whole-genome sequencing revealed that four of the five suppressors harbored mutations in or near *prc* or *nlpI* (Fig. 2*C*). Prc is a periplasmic protease that, together with its partner protein NlpI, plays a major role in the turnover of the cell wall endopeptidase MepS, which functions as a space-maker enzyme for cell elongation (25, 26). Of the three suppressors mapping to the *prc* locus, *prc*(ΔKNEA) encodes a short in-frame deletion of four residues (K157-A160) within the N-terminal helix domain of Prc, and *prc*(Y366C) results in a substitution of a residue near the flexible hinge located between the substrate-recognition PDZ domain and catalytic platform domain of the protease (27). The third allele results in a frameshift in the upstream *proQ* gene that we suspect is polar on *prc* expression. The suppressor in *nlpI*, *nlpI*(Q108P), results in an amino acid substitution in a helix directly apposing the Prc-interaction site (27). The fifth suppressor mapped to *secA*, which encodes an essential component of the Sec translocon. We focused the remainder of this study on the suppressors in *prc*.

The suppressing activity of the *prc*(ΔKNEA) and *prc*(Y366A) alleles was confirmed by transducing them into the parental background (*SI Appendix*, Fig. S3). To determine whether complete inactivation of Prc would also suppress the Tol-Pal defect, we constructed a Δ*prc* Δ*tol-pal* strain. This mutant unexpectedly remained incapable of growth on LB0N at 42 °C. We suspected that this lack of suppression may be due to the hyperaccumulation of MepS in the absence of Prc (26). Accordingly, the combination of Δ*mepS* and Δ*prc* alleles suppressed the growth and division defects of the Δ*tol-pal* mutant on LB0N at 42 °C (*SI Appendix*, Fig. S4). Based on these results, we infer that the suppressing activity of *prc* mutants in the Δ*tol-pal* background is likely due to the accumulation of one or more Prc substrates other than MepS.

Overexpression of PG Glycan-Cleaving Enzymes Suppresses the Δ*tol-pal* Division Defect. We reasoned that a multicopy suppressor analysis would reveal the identity of the putative Prc substrates promoting

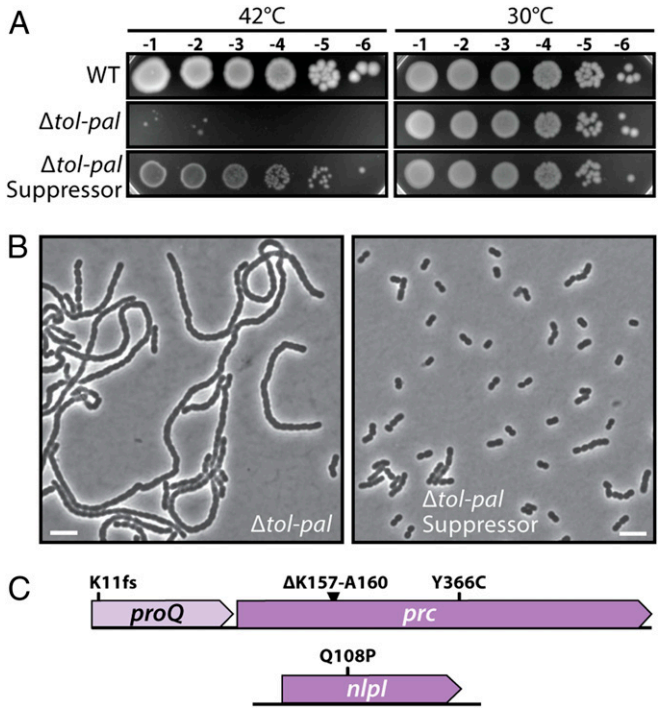

Fig. 2. Growth and division defects of a Δ*tol-pal* mutant are suppressed by mutations in *prc* and *nlpI*. (*A*) Serial dilutions of TB28 (WT), MT91 (Δ*tol-pal*), and a representative MT91 suppressor mutant *prc(Y366C)* were spotted on LB0N agar and grown at the indicated temperature. (*B*) Phase-contrast images of MT91 [Δ*tol-pal*] and a representative MT91 suppressor mutant grown in LB0N at 42 °C for 3 h. (Scale bars: 5 μm.) (*C*) Schematic showing the location of suppressor mutations.

cell division in the Δ*tol-pal* suppressors. Therefore, a library of plasmids encoding random 1- to 4-kb fragments of the *E. coli* chromosome was transformed into the *tol-pal* deletion strain. Transformants capable of growth on LB0N at 42 °C were selected and then screened by microscopy for those that corrected the Δ*tol-pal* division phenotype. Two clones were identified that suppressed the growth and division phenotype of the Δ*tol-pal* mutant: one containing a genomic region that included *mltB* and the other a region encoding the *yddW* gene. These genes, along with their upstream regions, were individually amplified and inserted into the parent vector of the multicopy library. Both constructs retained suppression activity for growth and division on LB0N at 42 °C (Fig. 3) and led to a modest increase in vancomycin resistance (*SI Appendix*, Fig. S5). Therefore, we conclude that overexpression of *mltB* or *yddW* alleviates several of the Δ*tol-pal* mutant phenotypes. However, the suppressed cells continue to produce OM vesicles when grown in minimal medium (*SI Appendix*, Fig. S6). These cells also display an accumulation of periplasmic GFP at midcell, which indicates a greater distance between the IM and OM at septa likely due to delayed OM constriction (28). Thus, despite their much-improved growth and division, problems with OM stability and constriction persist in the suppressed cells.

MltB is an OM lipoprotein with lytic transglycosylase (LT) activity (29). This class of enzymes cleaves the glycan chains of PG, generating a product with a 1,6-anhydro-*N*-acetylmuramic acid (MurNAc) moiety (30). Overexpression of a catalytically inactive derivative MltB(E162Q) failed to promote growth of the Δ*tol-pal* mutant on LB0N at 42 °C (*SI Appendix*, Fig. S7*A*), indicating that LT activity is required for suppression. To determine whether other LT enzymes were capable of suppressing the Tol-Pal defect, we overproduced several additional LTs in the mutant background. Two of the eight additional LTs tested, MltD or MltF, promoted the growth of the Δ*tol-pal* strain on LB0N at 42 °C (*SI Appendix*, Fig. S7*B*). Additionally, MltD overexpression substantially enhanced the vancomycin resistance of the mutant, indicating a partial restoration of OM permeability barrier (*SI Appendix*, Fig. S7*C*). From these results, we infer that the cell chaining defect following Tol-Pal inactivation can be suppressed by the overproduction of several different glycan-cleaving enzymes.

YddW (DigH) Is a Glycosyl Hydrolase. YddW is annotated as an *E. coli* protein of unknown function. It is predicted to be an OM lipoprotein with a Glycosyl Hydrolase-Like 10 (GHL10) domain (Fig. 4*A*). Using a cytological plasmolysis assay (31), we were able

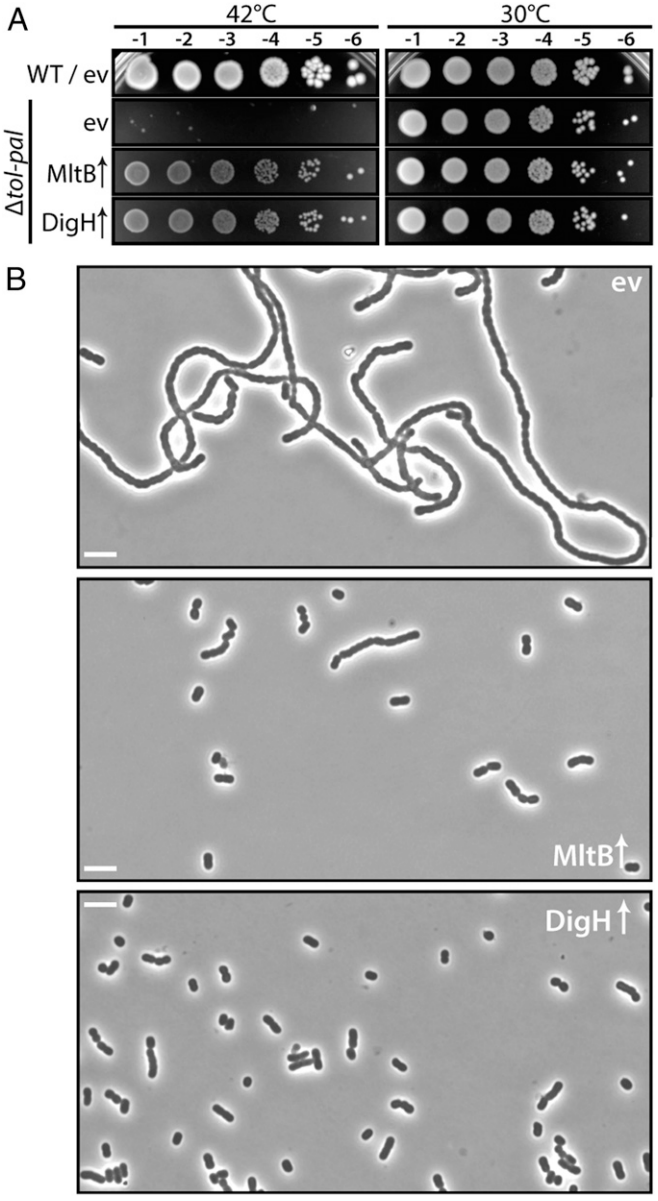

Fig. 3. Suppression of growth and division defects of a Δ*tol-pal* mutant by overexpression of MltB or DigH. (*A*) Serial dilutions of TB28 (WT) or MT91 (Δ*tol-pal*) harboring either the empty vector (ev) pCM6 or derivatives pAAY245 (*mltB*) or pAAY246 (*digH* [*yddW*]) harboring the indicated gene with its native upstream region for expression were spotted on LB0N agar and grown at the indicated temperature. (*B*) Phase-contrast images of MT91 cells with the same vectors following growth at 42 °C for 3 h. (Scale bars: 5 μm.)

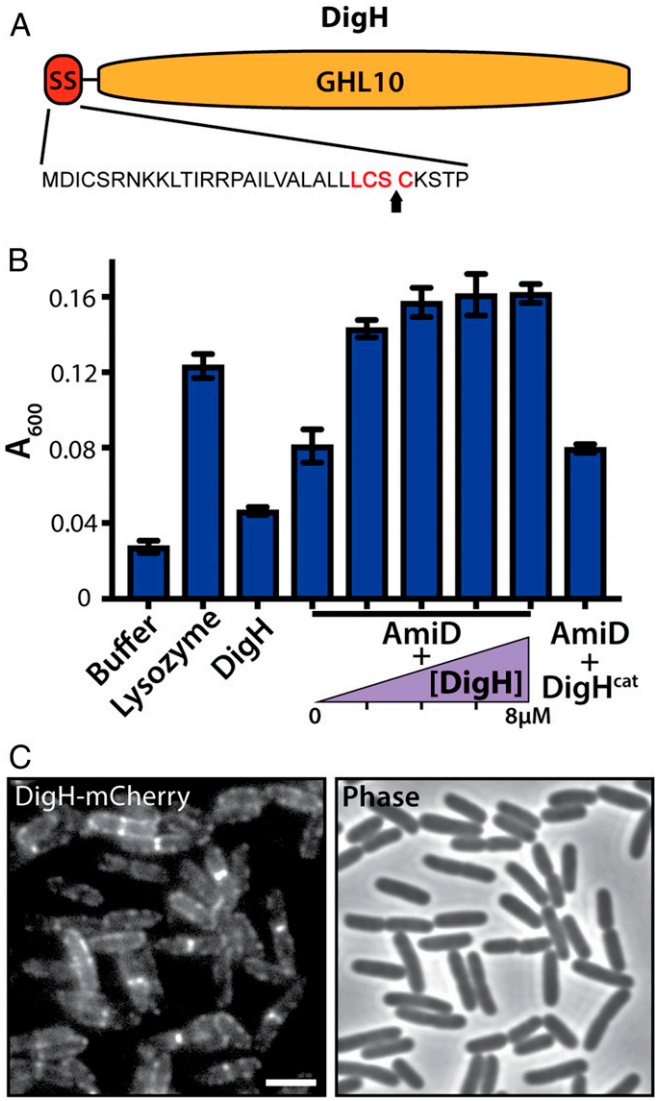

Fig. 4. Evidence that DigH is a glycosyl hydrolase that cleaves denuded peptidoglycan. (*A*) Schematic of the domain organization of DigH highlighting its single GHL10 domain and predicted lipoprotein signal sequence. The putative lipobox is indicated in bold red letters, and the putative signal peptidase cut site is marked with an arrow. (*B*) RBB-labeled sacculi were incubated for ~24 h with 200 μg/mL lysozyme, 8 μM DigH, or 0.5 μM AmiD along with 0, 2, 4, 6, or 8 μM WT DigH or 8 μM DigH(D236N). Upon quenching of the reaction with ethanol, the undigested PG was pelleted and released material was quantified by measuring dye absorbance at 600 nm. Data for three technical replicates, with the error bars representing the SE are shown. (*C*) An overnight culture of AAY119(*att*λAAY264) (Δ*digH* [P_{lac}::*digH-mCherry*]) was diluted 1:2,000 in M9 medium supplemented with 0.2% maltose and 250 μM isopropyl beta-D-1-thiogalacactopyranoside (IPTG). Cells were grown for 5 h at 37 °C and then imaged on agarose pads by phase contrast and fluorescence microscopy. Midcell localization of DigH-mCherry was observed in 27.3 ± 4.8% cells (7 images analyzed, >200 cells each). (Scale bar: 3 μm.)

to confirm that it localizes to the OM (*SI Appendix*, Fig. S8). Based on the findings presented below, we have renamed the protein DigH for divisome-localized glycosyl hydrolase. DigH homologs are sparsely, but very widely, distributed throughout the bacterial domain (*SI Appendix*, Fig. S9). Moreover, an ortholog from *Clostridium difficile*, Cwp19, has recently been shown to possess LT activity (32). To investigate the potential PG cleavage activity of DigH, a soluble version of the protein was purified and incubated with dye-labeled PG sacculi (RBB-PG). No significant PG cleavage activity was detected (Fig. 4*B*). Because some glycan-cleaving enzymes are specific for peptide-free (denuded) PG (33, 34), we next tested whether DigH could enhance PG degradation in combination with the amidase AmiD. Indeed, greater PG cleavage activity was observed in the AmiD+DigH combination than with AmiD alone. Importantly, a D236N variant of DigH, which is predicted to be catalytically inactive based on the structure of Cwp19 (35), failed to enhance PG cleavage in combination with AmiD (Fig. 4*B*). Overexpression of this mutant also failed to restore growth and division of the Δ*tol-pal* cells on LB0N at 42 °C, indicating that, as with MltB, PG cleavage is a requirement for the suppression activity of DigH (*SI Appendix*, Fig. S7*A*).

To investigate the PG cleavage activity of DigH further, we used liquid chromatography and mass spectrometry (LC/MS) to analyze the products produced in reactions with unlabeled PG. A major DigH-dependent peak was observed in reactions containing AmiD that corresponded in mass to a disaccharide containing *N*-acetylglucosamine (GlcNAc) and MurNAc without a 1,6-anhydro linkage (*SI Appendix*, Fig. S10*A*). Thus, rather than functioning as an LT enzyme, DigH appears to be a denuded PG-specific hydrolase with either glucosaminidase or muramidase activity. A small fraction of the reaction products was found to be GlcNAc-1,6-anhydroMurNAc (*SI Appendix*, Fig. S10*B*), which would be produced by muramidase cleavage of denuded sacculi at glycan termini. We therefore currently favor a muramidase designation for DigH, but further biochemical analysis will be required to solidify this assignment.

MltB and DigH Accumulate in *prc* Mutants and Are Required for *tol-pal* Suppression. To investigate the potential connection between MltB, DigH, and Prc, we measured the steady-state levels of MltB and DigH in mutants lacking the Prc protease. Both PG-cleaving enzymes accumulated in cells inactivated for Prc, regardless of whether they possessed a functional Tol-Pal system (*SI Appendix*, Fig. S11*A*). The enzymes also accumulated in Δ*tol-pal* cells harboring the suppressors *prc*(ΔKNEA) or *prc*(Y366A), but to a lesser degree than Δ*prc*, indicating that the alleles are likely to be hypomorphic. Unexpectedly, accumulation of MltB and DigH in the Δ*prc* Δ*mepS* double deletion was also reduced relative to the single *prc* deletion (*SI Appendix*, Fig. S11*A*). This result suggests that the PG cleaving enzymes may be degraded by proteases other than Prc when MepS accumulation is prevented. Although the accumulation of MltB and DigH is more modest in the Δ*tol-pal* Δ*prc* Δ*mepS* background, inactivation of either enzyme results in a loss of suppression (*SI Appendix*, Fig. S11*B*). We therefore infer that the inactivation of Prc suppresses the Δ*tol-pal* growth and division defects due to the combined accumulation of MltB, DigH, and potentially other PG glycan-cleaving enzymes.

DigH Is Recruited to the Divisome Independently of Tol-Pal. Because denuded glycans are formed at the division site by the amidases (2), we tested whether DigH localizes to the cytokinetic ring. A functional DigH-mCherry fusion (*SI Appendix*, Fig. S12) displayed a patchy localization around the cell periphery in predivisional cells (Fig. 4*C*), a pattern that is typical of OM lipoproteins (36). In cells undergoing constriction, the fusion additionally showed a pronounced accumulation at midcell indicative of recruitment to the cytokinetic ring (Fig. 4*C*). This recruitment was independent of the Tol-Pal system, but required amidase activation at the division site, indicating a requirement for the production of denuded glycan strands (*SI Appendix*, Fig. S13).

***tol-pal* Mutants Fail to Process Denuded PG Glycans at the Septum.** The results with DigH suggested that *tol-pal* mutants might accumulate uncleaved denuded PG glycans at their septa that cause the chaining phenotype. To test this possibility, we took advantage of the ability of SPOR domains to bind denuded glycans (37, 38). An exported derivative of the FtsN SPOR domain fused to

mCherry was produced in WT and Δ*tol-pal* cells, and its localization was assessed by fluorescence microscopy. In both strains, the fusion was found to robustly localize to sites of cell division (Fig. 5). As expected, based on previous work (37), the SPOR-mCherry fusion failed to localize to the septa of a mutant lacking all three division amidases (*SI Appendix*, Fig. S14). We therefore conclude that amidase activity is functional in Δ*tol-pal* mutants, but that these cells are not capable of properly processing the denuded PG produced following amidase activation. Furthermore, we observed that production of the SPOR-mCherry fusion induced a mild chaining defect in WT cells, and that these cells also produced OM vesicles that emanate from septa much like Δ*tol-pal* cells (37). From this result, we infer that excess SPOR domain at the septum can impair the processing of denuded PG glycans, and that the resulting chaining defect can induce OM constriction defects reminiscent of a Tol-Pal defect.

The Tol-Pal System May Have Functions Beyond the Modulation of PG Binding by Pal. According to the prevailing model, the main physiological function of the Tol-Pal system is to modulate the TolB-Pal interaction to promote the efficient formation of OM-PG linkages at the division site (11, 20, 21). If this function were the only activity of the Tol-Pal system, then a mutant deleted for all of the *tol-pal* genes should have an equivalent phenotype to one deleted for *pal* alone. On the contrary, although a Δ*pal* mutant is impaired, it grows far better on LB0N at 42 °C than the complete *tol-pal* deletion (*SI Appendix*, Fig. S15). These results thus suggest that the TolQRA motor and TolB may play additional roles in the cell besides the recruitment of Pal to the division site to help anchor the OM to the PG layer.

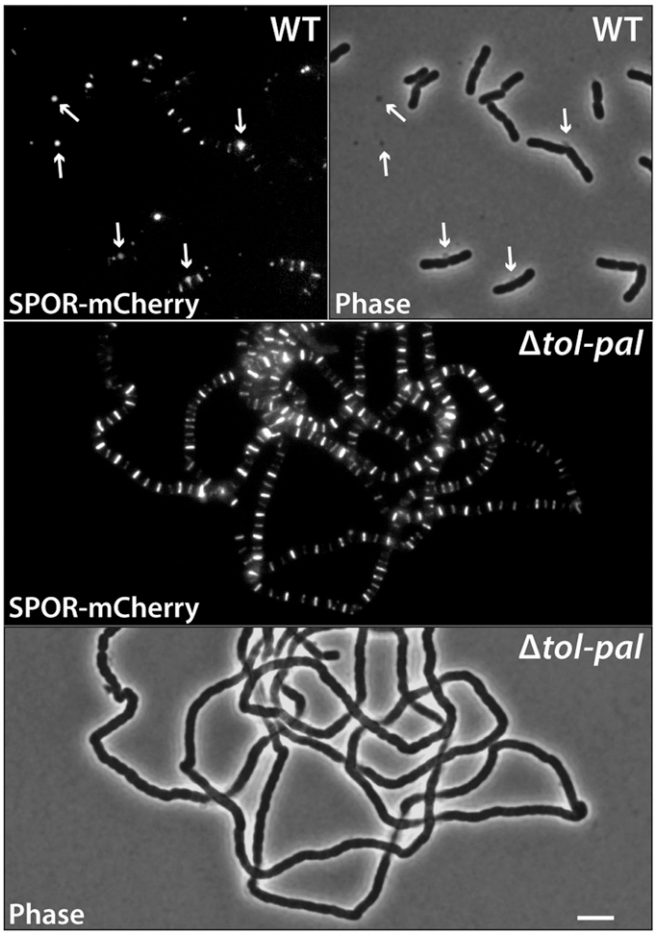

Fig. 5. SPOR domain localization in Δ*tol-pal* cells. Overnight cultures of TB28 (WT) and MT51 (Δ*tol-pal*) harboring the integrated expression construct *att*HKNP78 (P_{lac}::*dsbA*^{ss}-*mCherry-FtsN*^{SPOR}) were subcultured 1:2,000 in LB0N supplemented with 100 μM IPTG and grown for 2 h at 30 °C and then for 3 h at 42 °C. Cells were placed on agarose pads and imaged with phase contrast and epifluorescence optics. (Scale bar: 5 μm.) Arrows point to membrane blebs emanating from septa and mCherry-containing vesicles.

Discussion

It is widely believed that one of the primary functions of the Tol-Pal system is to promote OM constriction during cell division. This activity was initially proposed based on the observation that the machinery localizes to the division site, and that mutants defective for the system not only have a cell chaining phenotype, but also form OM blebs and vesicles that emanate from developing septa (11). Since its original description, the mechanistic model for how the Tol-Pal system might promote OM constriction has been revised significantly (21). According to current thinking, one of the key biochemical properties of the system is that the lipoprotein Pal can bind either TolB or the PG layer, but not both at the same time (39). By blocking PG binding, TolB association with Pal allows TolB-Pal complexes anchored to the to inner leaflet of the OM to diffuse throughout the cell periphery. When these complexes pass through the division site, the localized TolQRA motor is thought to bind TolB and use the proton motive force (PMF) (17) to break its tight association with Pal. Once the interaction is broken, OM-localized Pal is free to bind septal PG, thereby connecting the two envelope layers and promoting OM constriction (11, 20, 21).

Here, we show that in addition to linking the OM and PG layers, the Tol-Pal system is also required for the efficient processing of septal PG to complete the cell division process. The chaining phenotype in Δ*tol-pal* cells was found to be suppressed by the overexpression of one of several different PG glycan cleaving enzymes, suggesting that the mutant cells are largely connected by uncut glycans. Because the denuded glycan-specific hydrolase DigH was one of the enzymes capable of separating the chains of Δ*tol-pal* cells, the glycans linking the daughters must be at least partially denuded. Accordingly, the SPOR domain of FtsN, which binds denuded PG (38), was also found to accumulate at the incompletely processed septa of Tol-Pal defective cells. Denuded glycans are known to pose a significant impediment to the completion of cell division based on results from *Pseudomonas aeruginosa*, where inactivation of RlpA, a denuded glycan-specific LT, was shown to cause a cell chaining phenotype (34). From these results, we conclude that amidase activation remains functional when Tol-Pal is inactivated, but that the denuded glycan products produced are not efficiently processed and impair cell separation, presumably because they remain anchored at each end to opposite daughter poles (40). Thus, the chaining phenotype of *tol-pal* mutants cannot simply be interpreted as a defect in OM constriction. Additional roles for the complex during cell division related to septal PG remodeling must therefore be considered.

In *E. coli* and *Vibrio cholerae*, the deletion of multiple LT-encoding genes is required to generate a chaining phenotype that resembles the severity of the defect caused by inactivating Tol-Pal in these organisms (40, 41). Also, the inactivation of several LT enzymes in *P. aeruginosa* was found to compromise the OM permeability barrier (42). Thus, the activity of a number of different PG glycan cleaving enzymes is likely to be negatively impacted by disruption of Tol-Pal function to cause the chaining and OM barrier phenotypes. Because the vast majority of these enzymes are OM lipoproteins, the effect of Tol-Pal inactivation on their activity could be an indirect consequence of poor anchoring of the OM to the PG layer at the septum. One possibility is that increased distance between the PG and OM layers due to the anchoring defect causes the enzymes to have trouble reaching the substrate to cleave it. Alternatively, the release of OM vesicles from the septa

of *tol-pal* mutant cells might lead to a reduction in the number of enzymes available to carry out the septal remodeling process. However, we do not observe a significant reduction in either DigH or MltB levels in cells deleted for *tol-pal*. Also, if an increased OM-PG distance were the main cause of the PG remodeling defect, we would not expect overproduction of OM enzymes to overcome the distance barrier to correct the cell chaining defect induced by Tol-Pal inactivation. We therefore favor a model in which the Tol-Pal system plays a more direct role in promoting glycan cleavage at the division site by OM-localized enzymes. This activity could either be mediated through Pal binding to septal PG to alter its conformation and enhance cleavage, changes in PG cross-linking mediated by interactions of TolA and its partner CpoB with the PG synthase PBP1b (43), or via interactions between components of the Tol-Pal machinery and PG cleaving enzymes that stimulates their activity.

Although the mechanism by which the Tol-Pal system promotes efficient septal PG remodeling requires further investigation, our results clearly implicate the machinery in this process. Notably, mild Tol-Pal–like phenotypes, including cell chaining and OM bleb formation at septa, were observed upon overproduction of the FtsN SPOR domain. Binding of this domain to denuded glycans at septa presumably impairs their processing, raising the possibility that problems with PG remodeling generally contribute to some of the OM phenotypes observed for Tol-Pal defective cells. However, because suppression of the cell chaining defect of Tol-Pal inactivated cells did not correct all of their envelope-related issues, many of the known phenotypes for these mutants are likely to be unrelated to problems with septal PG processing. Importantly, similar to septal PG glycan cleavage, several of the other processes for which Tol-Pal has been implicated, like retrograde phospholipid transport (44, 45), utilize OM-lipoproteins. Moreover, our results indicate that inactivation of Pal does not result in a phenotype equivalent to removal of the entire machinery. Thus, although Pal is undoubtably the major substrate of the TolQRAB system due to its shear abundance (21), the system likely has functions unrelated to controlling the PG-binding properties of Pal. Given the growing number of connections between the Tol system and processes involving OM-lipoproteins, we propose that the system plays a more general role in modulating the activity of these factors than is currently appreciated, resulting in the pleiotropic phenotype displayed by *tol* mutants.

Materials and Methods

Data Availability Statement. All data supporting the conclusions drawn in this study in addition to the associated experimental protocols can be found in this report and *SI Appendix*. Research materials such as strains and plasmids are available upon request.

Strains, Media, and Strain Manipulation. *E. coli* cells were grown in LB (1% tryptone, 0.5% yeast extract, 0.5% NaCl), LB0N (LB lacking NaCl), or M9 medium supplemented with 0.2% casamino acids and 0.2% maltose. Unless noted otherwise, antibiotics were used at the following concentrations: ampicillin (Amp, 50 μg/mL), chloramphenicol (Cam, 25 μg/mL), kanamycin (Kan, 25 μg/mL), and tetracycline (Tet, 10 μg/mL). The strains and plasmids used in this study are listed in *SI Appendix*, Tables S1 and S2, respectively, and details of their construction can be found in the *SI Appendix* text.

Suppressor Selections. For selection of mutants that suppress Tol-Pal temperature sensitivity, isolated colonies of MT91 (Δ*tolQ-pal*) were grown overnight in LB at 30 °C in separate cultures. The cells were then washed twice with equal volume of LB0N, and 1:10 or 1:100 dilutions were plated on LB0N plates, which were incubated for 1 d at 42 °C. Surviving colonies were isolated, and suppression was confirmed by restreaking under the same restrictive condition. Mutations were mapped by whole-genome sequencing. For the multicopy suppressor selection, a multicopy plasmid library containing 1- to 4-kb chromosomal fragments (46) was electroporated into MT91 (Δ*tolQ-pal*) cells, and $>10^6$ transformants were selected on LB Cam plates at 30 °C. Cells in the resulting library were then selected for growth on LB0N supplemented with Cam, and plasmid inserts were identified by Sanger sequencing. See *SI Appendix* for details of the selection and sequencing methods used.

Viability Assays. For spot dilution assays, overnight cell cultures were typically subcultured 1:40 into LB medium and allowed to grow at 30 °C for 2 h. The cells were then washed with LB0N, normalized to OD_{600} of 1, and subjected to serial 10-fold dilutions with LB0N. Aliquots (5 μL) of the 10^{-1} to 10^{-6} dilutions were then spotted onto the plates indicated in the text, and the plates were incubated at the temperature indicated in figure legends for ∼24 h prior to imaging.

Protein Purification, Antibody Production, and Immunoblotting. Cytoplasmically expressed versions of His-SUMO–tagged MltB, DigH, and DigH(D236N) lacking their signal peptides were purified from BL21(λDE3) strain carrying pAAY277, pAAY251, or pAAY276, respectively. Details are provided in *SI Appendix*. For antibody generation, 625-μg samples of MltB and DigH were run on separate SDS/PAGE gels and stained with Coomassie. Bands corresponding to the proteins of interest were excised and subjected to custom antibody production protocol in rabbits by Covance Research Products. The specificity of the resulting sera was confirmed by immunoblotting of protein samples collected from WT cells and cells deleted for the respective gene. Immunoblotting procedures are detailed in *SI Appendix*.

PG Purification and Enzymatic Activity Assays. The PG sacculus purification protocol was adapted from Ursinus et al. (47). For the RBB dye release assay, PG sacculi were labeled with Remazol Brilliant Blue as previously described (10). Each reaction used 10 μL of labeled sacculi as the substrate and 50 mM Tris, pH 7.4., 0.5 μM purified AmiD (48), 200 μg/mL lysozyme (Sigma), and/or purified WT or catalytically dead DigH at the concentrations indicated in the text were also added. The reactions were incubated for ∼24 h at 37 °C and quenched by addition of ethanol to the final concentration of 33%. The samples were then centrifuged at 21,000 × g for 20 min, and the absorbance of the supernatant at 600 nm was measured with GloMax Explorer plate reader (Promega). LC-MS analysis was conducted following a previously described protocol (33), and details are provided in *SI Appendix*.

Microscopy. For morphological analysis of *tol-pal* suppressors, overnight cultures of cells were diluted 1:2,000 in LB0N and grown at 30 °C for 2 h and then at 42 °C for 3 h, the condition in which the cell division defect of *tol-pal* mutants is most severe. The cells were fixed with 2.5% formaldehyde and 0.04% glutaraldehyde in 60 mM sodium phosphate buffer, pH 7.4, for 20 min at room temperature and washed 2× with phosphate-buffered saline (PBS). Note that the cell division phenotype of *tol-pal* mutants was most severe when cells were grown at 42 °C, which is why morphological analysis was performed at this temperature. Growth conditions for the localization of fluorescent fusions an PG labeling are presented in the figure legends and detailed in *SI Appendix*.

ACKNOWLEDGMENTS. We thank all members of the T.G.B. and Rudner laboratories for advice and helpful discussions, Paula Montero-Lopez and the the MicRoN microscopy core for help with fluorescence microscopy, and the Harvard Center for Mass Spectrometry for help with peptidoglycan fragment analysis. This work was supported by National Institute of Allergy and Infections Diseases of the National Institutes of Health Grants R33 AI111713 and R01 AI083365 and funds from the Howard Hughes Medical Institute.

1. A. Typas, M. Banzhaf, C. A. Gross, W. Vollmer, From the regulation of peptidoglycan synthesis to bacterial growth and morphology. *Nat. Rev. Microbiol.* **10**, 123–136 (2011).
2. C. Heidrich *et al.*, Involvement of N-acetylmuramyl-L-alanine amidases in cell separation and antibiotic-induced autolysis of Escherichia coli. *Mol. Microbiol.* **41**, 167–178 (2001).
3. D. C. Yang, K. Tan, A. Joachimiak, T. G. Bernhardt, A conformational switch controls cell wall-remodelling enzymes required for bacterial cell division. *Mol. Microbiol.* **85**, 768–781 (2012).
4. A. J. F. Egan, Bacterial outer membrane constriction. *Mol. Microbiol.* **107**, 676–687 (2018).
5. E. F. Bi, J. Lutkenhaus, FtsZ ring structure associated with division in Escherichia coli. *Nature* **354**, 161–164 (1991).
6. A. W. Bisson-Filho *et al.*, Treadmilling by FtsZ filaments drives peptidoglycan synthesis and bacterial cell division. *Science* **355**, 739–743 (2017).
7. X. Yang *et al.*, GTPase activity-coupled treadmilling of the bacterial tubulin FtsZ organizes septal cell wall synthesis. *Science* **355**, 744–747 (2017).
8. J. Xiao, E. D. Goley, Redefining the roles of the FtsZ-ring in bacterial cytokinesis. *Curr. Opin. Microbiol.* **34**, 90–96 (2016).
9. T. Uehara, T. Dinh, T. G. Bernhardt, LytM-domain factors are required for daughter cell separation and rapid ampicillin-induced lysis in Escherichia coli. *J. Bacteriol.* **191**, 5094–5107 (2009).

10. T. Uehara, K. R. Parzych, T. Dinh, T. G. Bernhardt, Daughter cell separation is controlled by cytokinetic ring-activated cell wall hydrolysis. *EMBO J.* **29**, 1412–1422 (2010).
11. M. A. Gerding, Y. Ogata, N. D. Pecora, H. Niki, P. A. J. de Boer, The trans-envelope Tol-Pal complex is part of the cell division machinery and required for proper outer-membrane invagination during cell constriction in E. coli. *Mol. Microbiol.* **63**, 1008–1025 (2007).
12. E. Cascales *et al*., Colicin biology. *Microbiol. Mol. Biol. Rev.* **71**, 158–229 (2007).
13. A. Bernadac, M. Gavioli, J. C. Lazzaroni, S. Raina, R. Lloubès, Escherichia coli tol-pal mutants form outer membrane vesicles. *J. Bacteriol.* **180**, 4872–4878 (1998).
14. R. Lloubès *et al*., The Tol-Pal proteins of the Escherichia coli cell envelope: An energized system required for outer membrane integrity? *Res. Microbiol.* **152**, 523–529 (2001).
15. M. A. Llamas, J. L. Ramos, J. J. Rodríguez-Herva, Mutations in each of the tol genes of Pseudomonas putida reveal that they are critical for maintenance of outer membrane stability. *J. Bacteriol.* **182**, 4764–4772 (2000).
16. A. J. Heilpern, M. K. Waldor, CTXphi infection of Vibrio cholerae requires the tolQRA gene products. *J. Bacteriol.* **182**, 1739–1747 (2000).
17. E. Cascales, M. Gavioli, J. N. Sturgis, R. Lloubès, Proton motive force drives the interaction of the inner membrane TolA and outer membrane pal proteins in Escherichia coli. *Mol. Microbiol.* **38**, 904–915 (2000).
18. J. Meury, G. Devilliers, Impairment of cell division in tolA mutants of Escherichia coli at low and high medium osmolarities. *Biol. Cell* **91**, 67–75 (1999).
19. J.-F. Dubuisson, A. Vianney, N. Hugouvieux-Cotte-Pattat, J.-C. Lazzaroni, Tol-Pal proteins are critical cell envelope components of Erwinia chrysanthemi affecting cell morphology and virulence. *Microbiology* **151**, 3337–3347 (2005).
20. M. Petiti *et al*., Tol energy-driven localization of pal and anchoring to the peptidoglycan promote outer-membrane constriction. *J. Mol. Biol.* **431**, 3275–3288 (2019).
21. J. Szczepaniak *et al*., Pal stabilizes the bacterial outer membrane during constriction by a mobilisation-and-capture mechanism. *Nat. Commun.* (2020), in press.
22. M.-J. Tsang, A. A. Yakhnina, T. G. Bernhardt, NlpD links cell wall remodeling and outer membrane invagination during cytokinesis in Escherichia coli. *PLoS Genet.* **13**, e1006888 (2017).
23. H. Kowata, S. Tochigi, T. Kusano, S. Kojima, Quantitative measurement of the outer membrane permeability in Escherichia coli lpp and tol-pal mutants defines the significance of Tol-Pal function for maintaining drug resistance. *J. Antibiot. (Tokyo)* **69**, 863–870 (2016).
24. E. Kuru *et al*., In situ probing of newly synthesized peptidoglycan in live bacteria with fluorescent D-amino acids. *Angew. Chem. Int. Ed. Engl.* **51**, 12519–12523 (2012).
25. S. K. Singh, L. SaiSree, R. N. Amrutha, M. Reddy, Three redundant murein endopeptidases catalyse an essential cleavage step in peptidoglycan synthesis of Escherichia coli K12. *Mol. Microbiol.* **86**, 1036–1051 (2012).
26. S. K. Singh, S. Parveen, L. SaiSree, M. Reddy, Regulated proteolysis of a cross-link-specific peptidoglycan hydrolase contributes to bacterial morphogenesis. *Proc. Natl. Acad. Sci. U.S.A.* **112**, 10956–10961 (2015).
27. M.-Y. Su *et al*., Structural basis of adaptor-mediated protein degradation by the tail-specific PDZ-protease Prc. *Nat. Commun.* **8**, 1516 (2017).
28. T. G. Bernhardt, P. A. J. de Boer, Screening for synthetic lethal mutants in Escherichia coli and identification of EnvC (YibP) as a periplasmic septal ring factor with murein hydrolase activity. *Mol. Microbiol.* **52**, 1255–1269 (2004).
29. K. Ehlert, J. V. Höltje, M. F. Templin, Cloning and expression of a murein hydrolase lipoprotein from Escherichia coli. *Mol. Microbiol.* **16**, 761–768 (1995).
30. J. van Heijenoort, Peptidoglycan hydrolases of Escherichia coli. *Microbiol. Mol. Biol. Rev.* **75**, 636–663 (2011).
31. S. Lewenza, D. Vidal-Ingigliardi, A. P. Pugsley, Direct visualization of red fluorescent lipoproteins indicates conservation of the membrane sorting rules in the family Enterobacteriaceae. *J. Bacteriol.* **188**, 3516–3524 (2006).
32. S. Wydau-Dematteis *et al*., Cwp19 is a novel lytic transglycosylase involved in stationary-phase Autolysis resulting in toxin release in *Clostridium difficile*. *MBio* **9**, 1539 (2018).
33. C. Morlot, T. Uehara, K. A. Marquis, T. G. Bernhardt, D. Z. Rudner, A highly coordinated cell wall degradation machine governs spore morphogenesis in Bacillus subtilis. *Genes Dev.* **24**, 411–422 (2010).
34. M. A. Jorgenson, Y. Chen, A. Yahashiri, D. L. Popham, D. S. Weiss, The bacterial septal ring protein RlpA is a lytic transglycosylase that contributes to rod shape and daughter cell separation in Pseudomonas aeruginosa. *Mol. Microbiol.* **93**, 113–128 (2014).
35. W. J. Bradshaw, J. M. Kirby, A. K. Roberts, C. C. Shone, K. R. Acharya, The molecular structure of the glycoside hydrolase domain of Cwp19 from Clostridium difficile. *FEBS J.* **284**, 4343–4357 (2017).
36. C. Paradis-Bleau *et al*., Lipoprotein cofactors located in the outer membrane activate bacterial cell wall polymerases. *Cell* **143**, 1110–1120 (2010).
37. M. A. Gerding *et al*., Self-enhanced accumulation of FtsN at division sites and roles for other proteins with a SPOR domain (DamX, DedD, and RlpA) in Escherichia coli cell constriction. *J. Bacteriol.* **191**, 7383–7401 (2009).
38. A. Yahashiri, M. A. Jorgenson, D. S. Weiss, The SPOR domain, a widely conserved peptidoglycan binding domain that targets proteins to the site of cell division. *J. Bacteriol.* **199**, e00118-17 (2017).
39. D. A. Bonsor *et al*., Allosteric beta-propeller signalling in TolB and its manipulation by translocating colicins. *EMBO J.* **28**, 2846–2857 (2009).
40. A. I. Weaver *et al*., Lytic transglycosylases RlpA and MltC assist in Vibrio cholerae daughter cell separation. *Mol. Microbiol.* **112**, 1100–1115 (2019).
41. C. Heidrich, A. Ursinus, J. Berger, H. Schwarz, J.-V. Höltje, Effects of multiple deletions of murein hydrolases on viability, septum cleavage, and sensitivity to large toxic molecules in Escherichia coli. *J. Bacteriol.* **184**, 6093–6099 (2002).
42. R. P. Lamers, U. T. Nguyen, Y. Nguyen, R. N. C. Buensuceso, L. L. Burrows, Loss of membrane-bound lytic transglycosylases increases outer membrane permeability and β-lactam sensitivity in Pseudomonas aeruginosa. *Microbiologyopen* **4**, 879–895 (2015).
43. A. N. Gray *et al*., Coordination of peptidoglycan synthesis and outer membrane constriction during Escherichia coli cell division. *elife* **4**, e07118 (2015).
44. J. C. Malinverni, T. J. Silhavy, An ABC transport system that maintains lipid asymmetry in the gram-negative outer membrane. *Proc. Natl. Acad. Sci. U.S.A.* **106**, 8009–8014 (2009).
45. R. Shrivastava, X. Jiang, S.-S. Chng, Outer membrane lipid homeostasis via retrograde phospholipid transport in Escherichia coli. *Mol. Microbiol.* **106**, 395–408 (2017).
46. R. Yunck, H. Cho, T. G. Bernhardt, Identification of MltG as a potential terminase for peptidoglycan polymerization in bacteria. *Mol. Microbiol.* **99**, 700–718 (2016).
47. A. Ursinus *et al*., Murein (peptidoglycan) binding property of the essential cell division protein FtsN from Escherichia coli. *J. Bacteriol.* **186**, 6728–6737 (2004).
48. T. Uehara, J. T. Park, An anhydro-N-acetylmuramyl-L-alanine amidase with broad specificity tethered to the outer membrane of Escherichia coli. *J. Bacteriol.* **189**, 5634–5641 (2007).